Springer

Journal of
Mechanical
Science and
Technology

Journal of Mechanical Science and Technology 23 (2009) 1075~1082

www.springerlink.com/content/1738-494x
DOI 10.1007/s12206-009-0344-1

Sensitivity of a vehicle ride to the suspension bushing characteristics †

Jorge Ambrósio* and Paulo Verissimo

IDMEC-IST, Instituto Superior Técnico, Technical University of Lisbon, Av. Rovisco Pais, 1049-001 Lisboa, Portugal

(Manuscript Received December 24, 2008; Revised March 16, 2009; Accepted March 16, 2009)

Abstract

The sensitivity of the ride characteristics of a road vehicle to the mechanical characteristics of the bushings used in its suspension is discussed here. First, the development and computational implementation, on a multibody dynamics environment, of a constitutive relation to model bushing elements associated with mechanical joints is presented. Bushings are made of a rubber type of material, which presents a nonlinear and viscoelastic relationship between the forces and moments and their corresponding displacements and rotations. Suitable bushing models for vehicle multibody models must be accurate and computationally efficient, leading to more reliable models. The bushing is modeled in a multibody code as an arrangement of springs that penalize the motion between the bodies connected. In the methodology proposed here, a finite element model of the bushing is developed in the framework of a finite element (FE) code to obtain the curves of displacement/rotation versus force/moment for different loading cases. The basic ingredients of the multibody model are the same vectors and points relations used to define kinematic constraints in any multibody formulation. Spherical, cylindrical and revolute bushing joints are developed and implemented in this work, since the methodology is demonstrated through the ride over bumps, at different speeds, of two multibody models of a road vehicle: one with perfect kinematic joints, for the suspension sub-systems; the other with bushing joints, riding. Then, sensitivities of different vehicle kinematic responses to the characteristics of the bushings used in the suspension are evaluated, by using numerical sensitivities. Based on the sensitivity analysis, indications on how to modify the vehicle response by modifying the bushing characteristics are drawn.

Keywords: Elastometer models; Kinematic joint modeling; Multibody dynamics; Sensitivity analysis; Vehicle dynamics

1. Introduction

Road and railway vehicles must comply with a large spectrum of objectives including noise reduction, ride enhancement, dynamic behavior and/or handling improvement while reducing costs. Even after the vehicle is commercialized it may be necessary to fine-tune suspensions and other functional systems. The tools and models used in the vehicles design remain valuable for their evolution during their life.

The multibody code DAP3D, based in the multibody methodology proposed by Nikravesh [1], is used for the developments reported in this work. In this program the kinematic joints are modeled as perfect joints, i.e., the clearance existent in real joints or the possibility of the use of deformable elements, such as bushing elements, is not taken into account. However, clearance in the joints can be easily accommodated as shown in the work by Flores et al.[2].

The bushing elements are important in the vehicles' dynamic behavior because they handle misalignments between the suspension components, absorb vibrations and decrease the transmissibility of the road irregularities to the vehicle occupants. Their drawback is to increase the under-steering tendency and a less responsive vehicle [3]. Elastic bushings for multibody systems, consisting of linear springs to describe the elastic behavior of the elastomer bushing,

† This paper was presented at the 4th Asian Conference on Multibody Dynamics(ACMD2008), Jeju, Korea, August 20-23, 2008.

* Corresponding author. Tel.: +351 218417680, Fax.: +351 218417915
E-mail address: jorge@dem.ist.utl.pt

have been presented [4]. Since the bushing is a nonlinear elastic elastomer [5], different nonlinear viscoelastic bushings, providing accurate prediction of dynamic loads and displacements, are proposed [6]. This methodology consists in the assumption that the relaxation function can be expressed as a sum of nonlinear deformation functions that are exponentially decreasing in time. Modeling the bushings as sets of nonlinear viscoelastic forces, which depend not only on the instantaneous bushing deformations but also on their history, leads to heavy computational costs that are not compatible with their application to complex vehicle models.

In this study a methodology to model several types of nonlinear elastic bushings with stiffness proportional damping is presented, so that the sensitivity analysis can use, explicitly, the geometrical and material characteristics of these elements. The constitutive equations for the bushing joints are obtained through a detailed finite element analysis using a nonlinear finite element code. The bushing joints are implemented in the DAP3D multibody code. The influence of the bushing elements over the vehicle dynamics and the sensitivity of the vehicle response to the bushing characteristics was studied through the dynamic simulations of two vehicle multibody models, one with perfect joints and the other with bushing joints.

2. Bushing joints

Bushings joints are modeled as force arrangements that penalize the relative motion between the bodies connected. With different spring and damper arrangements most joints with bushings can be modeled. A straightforward computational procedure to develop the bushing models, based on the bushing model proposed by Ambrosio and Verissimo [7], is overviewed and demonstrated here through their application in vehicle dynamics applications.

The equations of motion of a multibody system and the second time derivative of constraint equations are,

$$\begin{bmatrix} \mathbf{M} & \boldsymbol{\Phi}_{\mathbf{q}}^{T} \\ \boldsymbol{\Phi}_{\mathbf{q}} & \mathbf{0} \end{bmatrix} \begin{Bmatrix} \ddot{\mathbf{q}} \\ \boldsymbol{\lambda} \end{Bmatrix} = \begin{Bmatrix} \mathbf{g} \\ \boldsymbol{\gamma} \end{Bmatrix} \tag{1}$$

where $\mathbf{M}$ is the mass matrix, $\ddot{\mathbf{q}}$ is the vector of the system accelerations, $\mathbf{g}$ is the force vector, $\boldsymbol{\Phi}_{\mathbf{q}}$ is the Jacobian matrix associated to the kinematic constraints, $\boldsymbol{\lambda}$ is the vector of Lagrange multipliers, which are related to the joint reaction forces, and $\boldsymbol{\gamma}$ is the right-hand-side of the acceleration constraint equations. The ideal kinematic constraints are included in the acceleration constraint equations, while the bushing joints are included in the force vector.

For the ideal kinematic joints, included in Eq. (1), the joint reaction forces of a particular joint over the connected bodies *i* and *j* are given by

$$\begin{aligned} \mathbf{f}_i &= -\boldsymbol{\Phi}_{\mathbf{q}_i}^{(t,n)} \boldsymbol{\lambda}^{(t,n)} \\ \mathbf{f}_j &= -\mathbf{f}_i \end{aligned} \tag{2}$$

where *t* refers to the type of joint and *n* is the number of constraints imposed by such joint. Note that Eq. (2) is included in the first line of Eq. (1). The principle of the development of the bushing joint forces is to substitute the joint reaction force described by Eq. (2) by a force given by the bushing.

It has been noted that using bushing joints instead of ideal kinematic joints in general multibody systems reduces the computational costs associated to the simulation of complex models. This is not unexpected since the use of bushing joints reduces the number of kinematic constraints required for the construction of a multibody model. Consequently, the fulfillment of the kinematic constraints is more easily achieved and the size of the integration time steps, selected by the numerical integrator of the equations of motion, used during the numerical integration is larger leading to faster computation times. However, for stiffer bushings, or for compliances with particular nonlinear constitutive laws, this trend may not apply due to the high frequency contents that they bring into the multibody system response.

2.1 Spherical bushing joint

The spherical joint allows for three free rotations between the bodies connected, penalizing only the relative translation displacements. A set of translational springs is used to represent the spherical bushing and limit the relative motion of the bodies connected, as presented in Fig. 1. The bushing reaction forces over bodies *i* and *j* are represented as

$$\begin{aligned} \mathbf{f}_i &= [K(\delta)\Delta\delta + f(\delta) + b\dot{\delta}]\frac{1}{d}\mathbf{d} \\ \mathbf{f}_j &= -\mathbf{f}_i \end{aligned} \tag{3}$$

where $K(\delta)\Delta\delta$ is the spring nonlinear elastic force increment, $f(\delta)$ represents the equivalent spring force due to its state of deformation, b is the stiffness proportional damping, and δ is the bushing deformation.

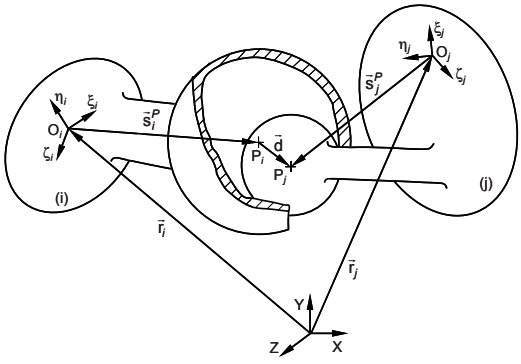

Fig. 1. Spherical bushing joint.

Vector **d**, is the distance between P_i and P_j, as

$$\mathbf{d} = \mathbf{r}_j + \mathbf{s}_j^P - \mathbf{r}_i - \mathbf{s}_i^P \tag{4}$$

and d is the length of vector **d** given by $d = \sqrt{\mathbf{d}^T\mathbf{d}}$ while $\dot{\delta}$ is the time rate of change of δ. Note that the difference between d and δ is simply a shift that accounts for the undeformed thickness of the bushing. When no gap exists between the two bodies involved in the joint $d=\delta$.

Assuming that no gap exists in the joint, $d=\delta$, and, according to Fig. 1 the time derivative of δ is

$$\dot{\delta} = \frac{\mathbf{d}^T\dot{\mathbf{d}}}{\delta} \tag{5}$$

where $\dot{\mathbf{d}}$ is the time derivative of Eq. (4) as

$$\dot{\mathbf{d}} = \dot{\mathbf{r}}_j + \mathbf{A}_j\tilde{\boldsymbol{\omega}}_j\mathbf{s}_j^P - \dot{\mathbf{r}}_i - \mathbf{A}_i\tilde{\boldsymbol{\omega}}_i\mathbf{s}_i^P \tag{6}$$

where $\boldsymbol{\omega}$ is the angular velocity of body i. When the bushing joint is not located in the center of mass of the connected bodies the transport moments are

$$\begin{aligned}\mathbf{n}_i' &= \mathbf{A}_i^T\left(\tilde{\mathbf{s}}_i^P\mathbf{f}_i\right)\\ \mathbf{n}_j' &= \mathbf{A}_j^T\left(\tilde{\mathbf{s}}_j^P\mathbf{f}_j\right)\end{aligned} \tag{7}$$

where $\tilde{\mathbf{s}}_i^P$ is a skew-symmetric matrix made with the components of vector $\mathbf{s}_i^P$.

2.2 Cylindrical bushing joint

The degrees of freedom to be penalized by this joint are the normal translational displacement, $\mathbf{d}_n$, depicted in Fig. 2, and the angular displacement due to the misalignment of the vectors, presented in Fig. 3.

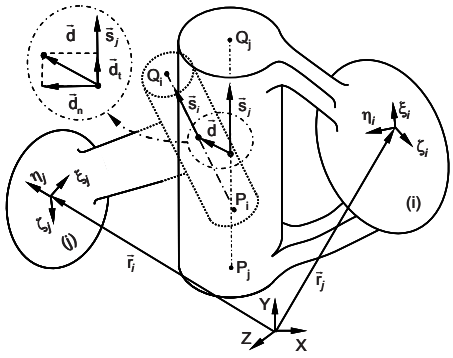

Fig. 2. Radial misalignment in the cylindrical, revolute and translation joints.

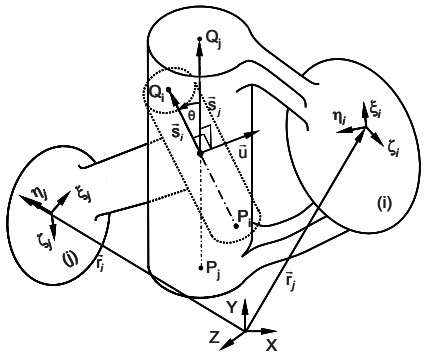

Fig. 3. Angular misalignment in the cylindrical, revolute and translation joints.

Based on Fig. 2 the misalignment of the axis of the joint in the tangential direction is given as

$$\mathbf{d}_t = \left(\mathbf{d}^T\mathbf{s}_j\right)\left(\mathbf{A}_j^T\mathbf{s}_j\right) \tag{8}$$

while the misalignment normal to the joint axis in body j is

$$\mathbf{d}_n = \mathbf{d} - \mathbf{d}_t \tag{9}$$

The unit vector $\mathbf{s}_i$ defines the joint axis in body i and the unit vector $\mathbf{s}_j$ defines the joint axis in body j.

The forces due to the normal misalignment of the axis are

$$\begin{aligned}\mathbf{f}_i &= [K(\delta_n)\Delta\delta_n + f(\delta_n) + b\dot{\delta}_n]\frac{1}{d_n}\mathbf{d}_n\\ \mathbf{f}_j &= -\mathbf{f}_i\end{aligned} \tag{10}$$

In Eq. (10) the magnitude of the deformation $\delta_n = \sqrt{\mathbf{d}_n^T\mathbf{d}_n}$ and the velocities $\dot{\delta}_n$ and $\dot{\delta}_t$ are

$$\dot{\delta}_n = \dot{\mathbf{d}}_n^T \mathbf{d}_n / \delta_n \tag{11}$$

$$\dot{\delta}_t = \dot{\mathbf{d}}_t^T \mathbf{d}_t / \delta_t \tag{12}$$

$$\dot{\mathbf{d}}_n = \dot{\mathbf{d}} - \dot{\mathbf{d}}_t \tag{13}$$

$$\dot{\mathbf{d}}_t = \left(\dot{\mathbf{d}}^T \mathbf{s}_j\right)\left(\mathbf{A}_j^T \mathbf{s}_j\right) \tag{14}$$

The moment due to the angular misalignment of vectors $\mathbf{s}_i$ and $\mathbf{s}_j$ requires calculating angle θ between them. First, let vector $\mathbf{u}$ be calculated as

$$\mathbf{u} = \tilde{\mathbf{s}}_i \mathbf{s}_j \tag{15}$$

then, using the definition of cross product, the misalignment angle in the revolute bushing joint is

$$\theta = \arcsin\left(|\mathbf{u}|\right) \tag{16}$$

where $|\mathbf{u}| = \sqrt{\mathbf{u}^T \mathbf{u}}$. The bushing misalignment moment is

$$\begin{aligned} \mathbf{n}_i' &= -[K(\theta)\Delta\theta + f(\theta) + b\dot{\theta})]\left(\mathbf{A}_i^T \mathbf{u}_M\right) \\ \mathbf{n}_j' &= [K(\theta)\Delta\theta + f(\theta) + b\dot{\theta})]\left(\mathbf{A}_j^T \mathbf{u}_M\right) \end{aligned} \tag{17}$$

where $\mathbf{u}_M = \mathbf{u}/|\mathbf{u}|$. The time derivative of Eq. (16) leads to

$$\dot{\theta} = \dot{u} \Big/ \sqrt{1-(u)^2} \tag{18}$$

where

$$\dot{u} = \mathbf{u}_M^T \dot{\mathbf{u}} \tag{18}$$

and

$$\dot{\mathbf{u}} = \left[\left(\mathbf{A}_j \boldsymbol{\omega}_j - \mathbf{A}_i \boldsymbol{\omega}_i\right)^T \mathbf{u}\right]\mathbf{u} \tag{19}$$

In Eq. (19) $\boldsymbol{\omega}$ is the body angular velocity. Note that the moment calculated by Eq. (17) must be added to the transport moment that results from using Eq. (7) on the bushing reaction forces given by Eq. (10).

The formulation proposed for the cylindrical bushing joint requires the knowledge of the joint position, P_i and P_j, the coordinates of points Q_i and Q_j, which defines the joint axis, defined in bodies i and j, respectively. The translational stiffness defined in the normal direction, $K(\delta_n)$, and the rotation stiffness $K(\theta)$, and their correspondent damping factors complete the full definition of the cylindrical bushing model input data.

2.3 Revolute bushing joint

The formulation for the bushing revolution joint is based on the bushing cylindrical joint, to which a penalization of the relative displacement in the direction of the joint axis is added. Based Fig. 2 this force is

$$\begin{aligned} \mathbf{f}_i &= [K(\delta_t)\Delta\delta_t + f(\delta_t) + b\dot{\delta}_t]\frac{\mathbf{d}_t}{d_t} \\ \mathbf{f}_j &= -\mathbf{f}_i \end{aligned} \tag{20}$$

The input for the revolute bushing joint is the same as the cylindrical joint, plus the stiffness defined in the tangential direction $K(\delta_t)$ and the corresponding damping coefficient b.

3. Constitutive equations for bushings

The models of the bushing joints require that their stiffness is defined. Because the bushings are rubber type materials, their stiffness is nonlinear and characterized by functions that need to be identified. For the purpose, four test cases were conducted in the finite element (FE) program ABAQUS [8] with an FE model of the bushing element. The bushing is modeled with 1404 solid "hybrid" elements denominated by C3D8H in the finite element code, as depicted in Fig. 4. A rigid discrete cylindrical plate is created and tied to the nodes of the outer surface. A fixed boundary condition is prescribed to nodes in the inner surface. By applying displacements or rotations in the external rigid plate and measuring the reaction force or moments, respectively, in the plate the nonlinear stiffness constitutive functions for the bushings are obtained.

The FE program used has several constitutive laws for nonlinear elastic and finite deformation analysis. A polynomial form of the material law is used for the force calculations, as it provides good prediction the experimental deformation values [5]. The Ogden form of the material law is used to evaluate the moments because it produces a better fit for small angles of rotation. The parameters values used for both constitutive laws are obtained from the reference [5].

The proportional stiffness damping factor, b, is assumed to be 0.01 for the normal and tangential direction and zero for the torsion stiffness. The transla-

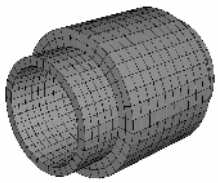

Fig. 4. Finite element mesh of the bushing model.

tional stiffness curve for a spherical bushing joint is presented in Fig. 5(b), where the damping factor, *b*, is assumed to be null.

4. Application to vehicle ride

The multibody model of a small family car, presented in Fig. 6, is used to present the developments reported in this paper and to serve as the object to carry the sensitivity analysis on the effect of the bushing properties on the vehicle dynamics. The data required to build the multibody model is obtained through direct measurement of the real vehicle components and, therefore, the manufacturer has no responsibility on the data presented or used here.

The vehicle front suspension is a McPherson mechanism, presented Fig. 7. In the rear suspension, presented in Fig. 8, a torsion beam suspension system is used, which is a common choice for this vehicle segment as it insures the compactness required for a small car while reducing the need for an anti-roll bar. However, the vehicle considered here still includes the anti-roll bar.

The inertia properties of the rigid body, center of mass location and body fixed frame orientations, and all data for the suspensions, tires and stabilization bars, are described in the work by Verissimo [9]. Two models of the vehicle are considered in the study that follows: one with ideal kinematic joints in the suspen-

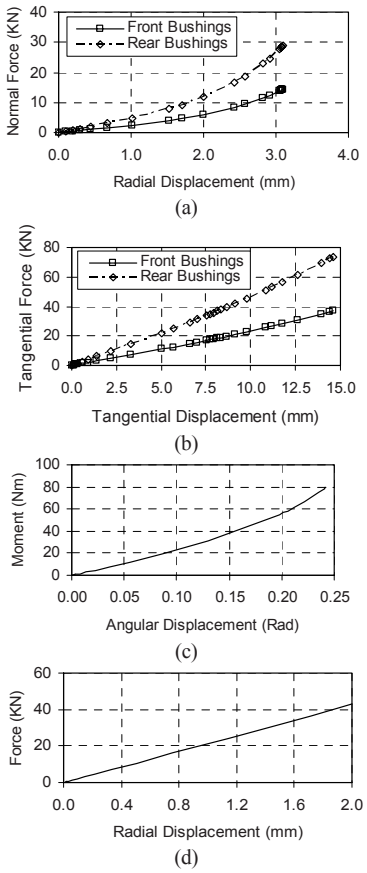

Fig. 5. Revolute bushing joints: (a) radial stiffness; (b) tangential stiffness; (c) torsional stiffness; (d) stiffness of the spherical bushing joint.

Fig. 6. Small family car modeled in this work.

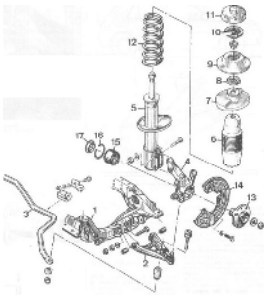

Fig. 7. Front suspension of the small family car.

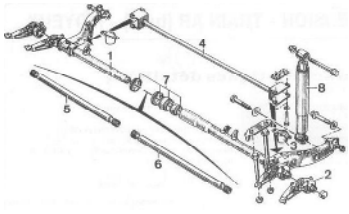

Legend:
1 – Axis
2 – Suspension Arm
3 – Clearance Limiter
4 – Stabilizer Bar
5 – Right Torsion Bar
6 – Left Torsion Bar
7 – Central Axis
8 – Damper

Fig. 8. Rear suspension of the small family car.

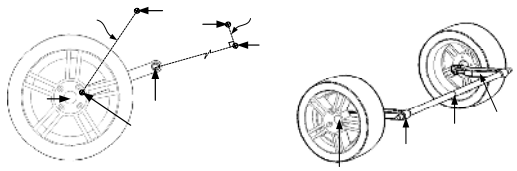

Fig. 9. Kinematic joints for the rear suspension: (a) model with ideal joints; (b) model with bushing joints.

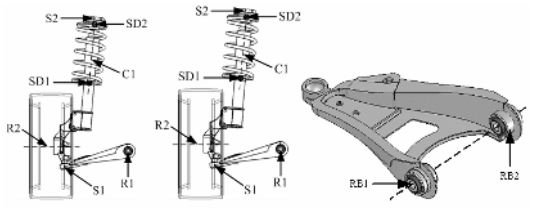

Fig. 10. Kinematic joints for the front suspension: (a) model with ideal joints; (b) model with bushing joints; (c) revolute bushing joints in the suspension arm.

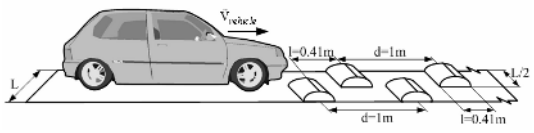

Fig. 11. Vehicle riding over bumps.

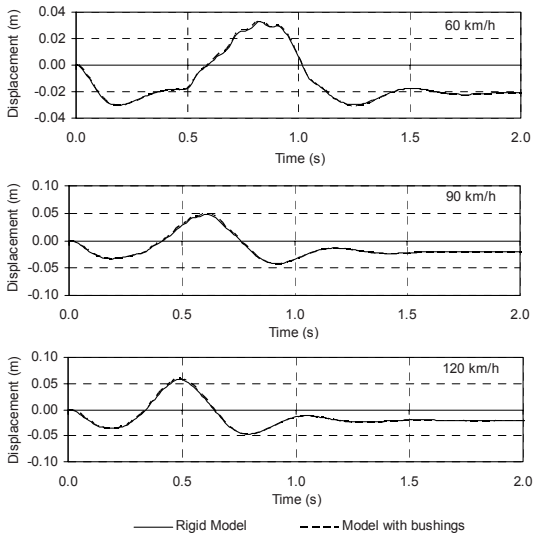

Fig. 12. Vertical displacement for the vehicle at different speeds: 60 km/h, 90 km/h, 120 km/h.

sion systems and another using bushing joint in selected suspension elements. The location of the bushing joints on the rear suspension system, referred to as *RB3*, is represented in Fig. 9.

The locations of the front suspension bushing joints are shown in Fig. 10(b) and c. The stiffness curves for the bushing joints model are obtained by a finite element model analysis, being the revolution bushing joints *RB1*, *RB2* and *RB3* the normal, tangential and rotational stiffness functions presented in Fig. 5.

The application scenario, represented in Fig. 11, considers the vehicle riding over ten bumps, with a height of 0.1m. This case excites the roll motion of

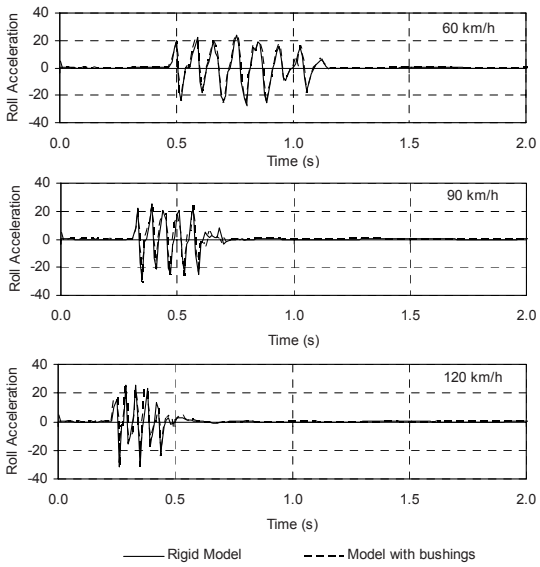

Fig. 13. Roll acceleration of the vehicle chassis for speeds of: 60 km/h, 90 km/h, 120 km/h.

the vehicle chassis, making possible an evaluation of the suspension efficiency to reduce this chassis motion. Forward vehicle speeds of 60, 90 and 120Km/h are used to study the case. The dynamic behavior of the vehicle models for this scenario can be characterized by its vertical position and by the roll accelerations, depicted in Figs. 12 and 13.

Analyzing the results presented in Fig. 12 for the vertical displacement of the center of mass of the chassis, it is observed that the vertical displacement is larger for the forward vehicle velocity of 120 km/h and smaller for the velocity of 60 km/h, as expected. The bushing joints present a relatively small influence on the vehicle dynamics. The roll acceleration response, depicted in Fig. 13, also shows slightly different dynamic behaviors for the two vehicle models. However, the model with bushing joints presents overall peak values smaller than the rigid model.

The deformations in a bushing joint for the scenario studied for a vehicle forward velocity of 90 Km/h, are presented in Fig. 14 for bushing joint *RB1*. The first peak shown must be disregarded as it is associated with the initial conditions of the simulation only. The peaks that follow are the displacements related to wheels hitting the bumps. The normal deformations reach 2.13 mm, while the tangential deformations reach 1.34 mm and the larger angular displacement value is 1.34 degrees.

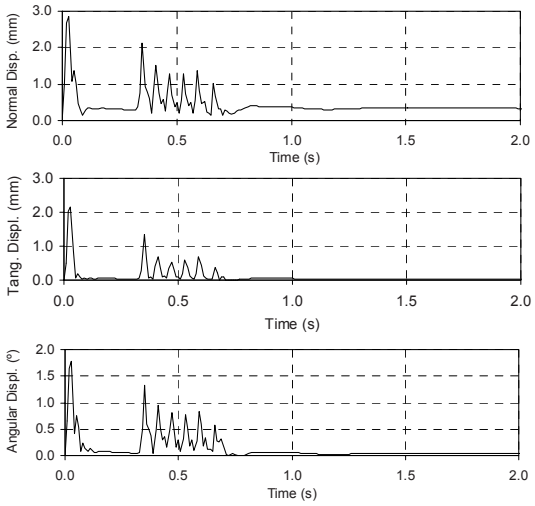

Fig. 14. Deformation of the bushing joint *RB1*: (a) radial; (b) tangential; (c) angular.

5. Sensitivity analysis

The sensitivity analysis provides information on how changes in the design variables influence the system performance. The sensitivities are calculated here by using the finite difference method [10, 11]. Neither the direct differentiation [12, 13] nor the adjoint variable methods [14] are used because require analytical evaluations of the sensitivities. The perturbations used for the finite difference sensitivities are selected in order to avoid truncation and round off numerical errors [14].

The stiffness functions, which represent the perturbed functions, are increased by 1% for the sensitivity calculations. It must be noted that the damping coefficients remain the same in the reference and perturbed cases, i.e., equal to 0.01.

The sensitivity analysis is performed to evaluate the influence of the bushing stiffness on the vehicle ride. The radial, tangential and angular stiffness represent independent design variables. The scenario in which the sensitivity analysis is carried consists in a vehicle traveling over several bumps with a forward speed of 90 km/h, as shown in Fig. 11. The reference functions for this scenario are the vertical position, vertical acceleration and roll acceleration of the vehicle chassis center of mass.

The sensitivity of the vertical position of the vehicle mass center is presented in Fig. 15. It is verified that the vertical position is very sensitive to changes of the normal front bushing stiffness. In this case it is

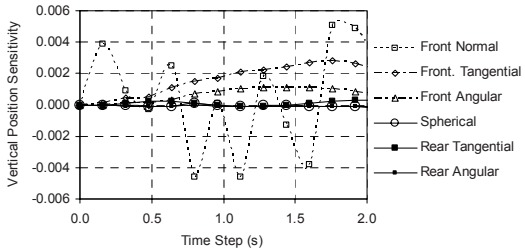

Fig. 15. Sensitivity of the vertical position of the vehicle center of mass.

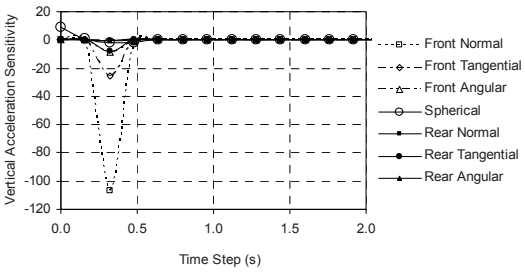

Fig. 16. Sensitivity of the vertical acceleration.

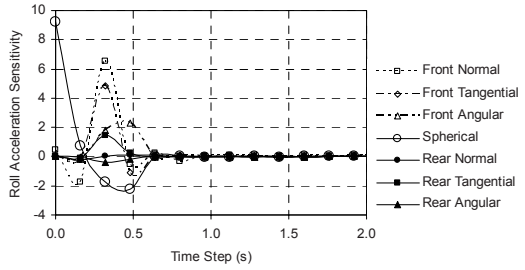

Fig. 17. Sensitivity of the roll acceleration.

verified that it is necessary the increase of the damping coefficient in order to obtain a smooth the dynamic response. Fig. 15 also shows that the vertical chassis position is more sensitive to the tangential front bushing stiffness, since that the sensitivity values are positive and higher in the entire simulation time domain. The angular front bushing stiffness has a smaller influence but it is still important to minimize the vertical position of the vehicle center of mass.

The sensitivity of the vertical acceleration of the chassis center of mass sensibility is presented in Fig. 16. It is observed that the stiffness of the front bushings is more influential on the vehicle vertical acceleration. For the minimization of the vehicle vertical acceleration it is more important the spherical bushing stiffness.

The sensitivity of the roll acceleration of the vehicle center of mass is depicted in Fig. 17. Here it is

shown that the rear bushing stiffness does not affect the vehicle chassis roll acceleration considerably. On the other hand, this motion characteristic is significantly affected by the front bushing stiffness.

In summary, the tangential stiffness for the front revolute bushing joints is more important to reduce the vertical displacement and the vertical and roll accelerations for the scenario simulated in this section. All other bushing joints play a relatively less important role.

6. Conclusions

A sensitivity analysis of the dynamics of a road vehicle due to variations of the characteristics of its bushing joints has been presented in this work. In the process a methodology to characterize and implement in a multibody environment models of bushing joints has been presented and demonstrated. The advantage of the formulation is that the usual kinematic quantities used to define ideal kinematic joints are still used here to define the relative orientation and displacement between the connected bodies. By applying the formulation to the ride of a vehicle over a series of bumps, the effect of the bushing stiffness on the vehicle dynamic response has been observed. From the results presented we conclude that the bushing joints of the front suspension are the most influential elements in modifying the vertical displacements and roll accelerations of the vehicle chassis.

References

[1] P. Nikravesh, *Computer-Aided Analysis of Mechanical Systems*, Prentice-Hall, Englewood Cliffs, New Jersey, USA (1988).

[2] P. Flores, J. Ambrósio, J. Pimenta Claro and H. Lankarani, *Kinematics and Dynamics of Multibody Systems with Imperfect Joints: Models and Case Studies*, Springer, Dordrecht, Netherlands, (2008).

[3] J. Park and P. Nikravesh, Effect of steering-housing rubber bushings on the handling responses of a vehicle. *SAE Transactions Journal of Passenger Cars*, 106(6) (1998) 76-86.

[4] J. Kang, J. Yun, J. Lee and T. Tak, Elastokinematic Analysis and Optimization of Suspension Compliance Characteristics, *Proceedings of Steering and suspensions technology*, SAE Paper 970104, SAE International, Warrendale, USA, (1997) 161-167.

[5] J. Kadlowec, A. Wineman and G. Hulbert, Elastomer bushing response: Experiments and finite element modeling. *Acta Mechanica*, 163 (2003) 25-38.

[6] R. Ledesma, Z. Ma, G. Hulbert and A. Wineman, A nonlinear viscoelastic bushing element in multibody dynamics, *Computational Mechanics*, 17 (1996) 287-296.

[7] J. Ambrosio and P. Verissimo, Improved bushing models for vehicle dynamics, *Multibody System Dynamics*, to be published (2009).

[8] Hibbitt, Karlsson & Sorensen, *ABAQUS User's Manual*, Pawtucket, Massachusetts, USA, (1999).

[9] P. Verissimo, *Improved Bushing Models for Vehicle Dynamics*, MSc. Thesis, Instituto Superior Técnico, Technical University of Lisbon, Portugal (2007).

[10] R. Hafka and H. Adelman, Recent developments in structural sensitivity analysis, *Structural Optimization*, 1 (1989) 137-151.

[11] D. Tortorelli and P. Michaleris, Design Sensitivity Analysis: Overview and Review, *Inverse Problems in Engineering*, 1 (1994) 71-105.

[12] P. Kirshnaswami and M. Bhatti, A general approach for design sensitivity analysis of constrained dynamic systems, *ASME* Paper 84-DET-132 (1984).

[13] J. Ambrósio, M. Augusta Neto and R.Leal, Optimization of a complex flexible multibody systems with composite materials, *Multibody Systems Dynamics*, 18(2) (2007) 117-144.

[14] J. Gonçalves, *Rigid and Flexible Multibody Systems Optimization for Vehicle Dynamics*, PhD Thesis, Instituto Superior Técnico, Technical University of Lisbon, Portugal (2002).

Jorge A.C. Ambrósio received his Ph.D. degree from the University of Arizona in 1991, being currently Professor at the Mechanical Engineering Department of Instituto Superior Técnico at the Technical University of Lisbon, Portugal. He is the author of several books and a large number of papers in international journals in the areas of multibody dynamics, vehicle Dynamics, crashworthiness and biomechanics. He has been responsible for several international projects in railway dynamics, biomechanics and passive safety. Currently he is the Editor-in-Chief of Multibody System Dynamics and member of the editorial boards of several international journals.